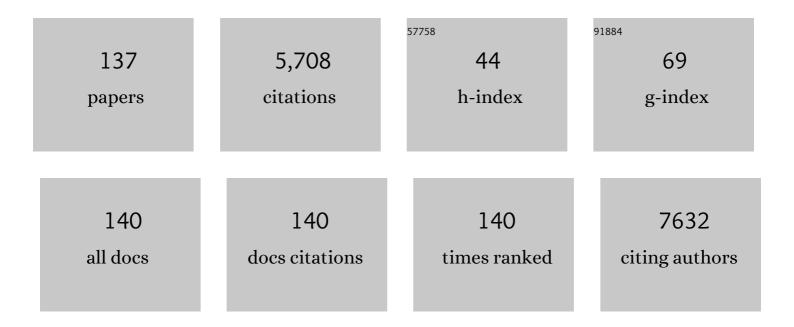
List of Publications by Year in descending order

Source: https://exaly.com/author-pdf/364866/publications.pdf Version: 2024-02-01



| #  | Article   | IF   | CITATIONS |
|----|---|------|-----------|
| 1  | Correlating the electronic structure of perovskite La1â^'Sr CoO3 with activity for the oxygen evolution reaction: The critical role of Co 3d hole state. Journal of Energy Chemistry, 2022, 65, 637-645.  | 12.9 | 39        |
| 2  | The role of the surface acidic/basic centers and redox sites on TiO2 in the photocatalytic CO2 reduction. Applied Catalysis B: Environmental, 2022, 303, 120931.  | 20.2 | 34        |
| 3  | Improved Methane Production by Photocatalytic CO2 Conversion over Ag/In2O3/TiO2 Heterojunctions.<br>Materials, 2022, 15, 843.   | 2.9  | 5         |
| 4  | Structural and electronic insight into the effect of indium doping on the photocatalytic performance of TiO <sub>2</sub> for CO <sub>2</sub> conversion. Journal of Materials Chemistry A, 2022, 10, 6054-6064.   | 10.3 | 13        |
| 5  | New Insight into Sorption Cycling Stability of Three Al-Based MOF Materials in Water Vapour.<br>Nanomaterials, 2022, 12, 2092.  | 4.1  | 1         |
| 6  | Unravelling nanostructured Nb-doped TiO <sub>2</sub> dual band behaviour in smart windows by<br><i>in situ</i> spectroscopies. Journal of Materials Chemistry A, 2022, 10, 19994-20004.   | 10.3 | 6         |
| 7  | One-Metal/Two-Ligand for Dual Activation Tandem Catalysis: Photoinduced Cu-Catalyzed<br>Anti-hydroboration of Alkynes. Journal of the American Chemical Society, 2022, 144, 13006-13017.  | 13.7 | 24        |
| 8  | Laser-Reduced BiVO <sub>4</sub> for Enhanced Photoelectrochemical Water Splitting. ACS Applied<br>Materials & Interfaces, 2022, 14, 33200-33210.  | 8.0  | 15        |
| 9  | Highly efficient multi-metal catalysts for carbon dioxide reduction prepared from atomically sequenced metal organic frameworks. Nano Research, 2021, 14, 493-500.  | 10.4 | 12        |
| 10 | Assessing the feasibility of reduced graphene oxide as an electronic promoter for photocatalytic hydrogen production over Nb-Ta perovskite photocatalysts. Catalysis Today, 2021, 362, 22-27.   | 4.4  | 9         |
| 11 | Selectivity in UV photocatalytic CO2 conversion over bare and silver-decorated niobium-tantalum perovskites. Catalysis Today, 2021, 361, 85-93.   | 4.4  | 17        |
| 12 | Macroscopic yarns of FeCl3-intercalated collapsed carbon nanotubes with high doping and stability.<br>Carbon, 2021, 173, 311-321.   | 10.3 | 14        |
| 13 | Self-supported ultra-active NiO-based electrocatalysts for the oxygen evolution reaction by solution combustion. Journal of Materials Chemistry A, 2021, 9, 12700-12710.  | 10.3 | 14        |
| 14 | The electronic structure of transition metal oxides for oxygen evolution reaction. Journal of Materials Chemistry A, 2021, 9, 19465-19488.  | 10.3 | 90        |
| 15 | Understanding ultrafast charge transfer processes in SnS and SnS <sub>2</sub> : using the core hole clock method to measure attosecond orbital-dependent electron delocalisation in semiconducting layered materials. Journal of Materials Chemistry C, 2021, 9, 11859-11872. | 5.5  | 5         |
| 16 | Tailoring the Electronic Structures of the La <sub>2</sub> NiMnO <sub>6</sub> Double Perovskite as Efficient Bifunctional Oxygen Electrocatalysis. Chemistry of Materials, 2021, 33, 2062-2071.   | 6.7  | 58        |
| 17 | lonic liquid-assisted synthesis of F-doped titanium dioxide nanomaterials with high surface area for<br>multi-functional catalytic and photocatalytic applications. Applied Catalysis A: General, 2021, 613,<br>118029.   | 4.3  | 14        |
| 18 | Photoâ€Induced Selfâ€Cleaning and Wettability in TiO <sub>2</sub> Nanocolumn Arrays Obtained by<br>Glancingâ€Angle Deposition with Sputtering. Advanced Sustainable Systems, 2021, 5, 2100071.  | 5.3  | 11        |

| #  | Article   | IF                       | CITATIONS                |
|----|---|--------------------------|--------------------------|
| 19 | Bringing Earth-Abundant Plasmonic Catalysis to Light: Gram-Scale Mechanochemical Synthesis and<br>Tuning of Activity by Dual Excitation of Antenna and Reactor Sites. ACS Sustainable Chemistry and<br>Engineering, 2021, 9, 9750-9760.                       | 6.7                      | 7                        |
| 20 | A molecular approach to the synthesis of platinum-decorated mesoporous graphitic carbon nitride as selective CO2 reduction photocatalyst. Journal of CO2 Utilization, 2021, 50, 101574.   | 6.8                      | 13                       |
| 21 | Conjugated Porous Polymers Based on BODIPY and BOPHY Dyes in Hybrid Heterojunctions for<br>Artificial Photosynthesis. Advanced Functional Materials, 2021, 31, 2105384.   | 14.9                     | 25                       |
| 22 | Conjugated Porous Polymers: Groundâ€Breaking Materials for Solar Energy Conversion. Advanced<br>Energy Materials, 2021, 11, 2101530.  | 19.5                     | 44                       |
| 23 | <mml:math<br>xmlns:mml="http://www.w3.org/1998/Math/MathML"&gt;<mml:msup><mml:mrow><mml:mi>Ni</mml:mi>-induced semiconductor-to-metal transition in spinel nickel cobaltite thin films. Physical Review B,<br/>2021, 104.</mml:mrow></mml:msup></mml:math<br> | 1row> <mr<br>3.2</mr<br> | nl:ŋrow> <m< td=""></m<> |
| 24 | TiO2-reduced graphene oxide-Pt nanocomposites for the photogeneration of hydrogen from ethanol liquid and gas phases. Catalysis Today, 2021, 380, 41-52.  | 4.4                      | 8                        |
| 25 | Heterogeneous photocatalysis. , 2021, , 1-38.   |                          | 0                        |
| 26 | Photoinduced Charge Transfer and Trapping on Single Gold Metal Nanoparticles on TiO <sub>2</sub> .<br>ACS Applied Materials & Interfaces, 2021, 13, 50531-50538.  | 8.0                      | 12                       |
| 27 | Metal-catalyst-free gas-phase synthesis of long-chain hydrocarbons. Nature Communications, 2021, 12, 5937.  | 12.8                     | 7                        |
| 28 | Recent Advances Towards Sustainable Materials and Processes for Energy Conversion and Storage.<br>Advanced Energy Materials, 2021, 11, 2102874.   | 19.5                     | 3                        |
| 29 | Controlled Synthesis of Up-Conversion NaYF4:Yb,Tm Nanoparticles for Drug Release under Near<br>IR-Light Therapy. Biomedicines, 2021, 9, 1953.   | 3.2                      | 2                        |
| 30 | Ferrite Materials for Photoassisted Environmental and Solar Fuels Applications. Topics in Current Chemistry, 2020, 378, 6.  | 5.8                      | 39                       |
| 31 | Fundamental Insights into Photoelectrocatalytic Hydrogen Production with a Hole-Transport<br>Bismuth Metal–Organic Framework. Journal of the American Chemical Society, 2020, 142, 318-326.   | 13.7                     | 60                       |
| 32 | Hybrids Based on BOPHY-Conjugated Porous Polymers as Photocatalysts for Hydrogen Production:<br>Insight into the Charge Transfer Pathway. ACS Catalysis, 2020, 10, 9804-9812.   | 11.2                     | 38                       |
| 33 | Exploring the alternative MnO-Na2CO3 thermochemical cycle for water splitting. Journal of CO2<br>Utilization, 2020, 42, 101264.   | 6.8                      | 9                        |
| 34 | Highly porous Ti–Ni anodes for electrochemical oxidations. Sustainable Energy and Fuels, 2020, 4,<br>4003-4007.   | 4.9                      | 1                        |
| 35 | Silver–Gold Bimetal-Loaded TiO <sub>2</sub> Photocatalysts for CO <sub>2</sub> Reduction.<br>Industrial & Engineering Chemistry Research, 2020, 59, 9440-9450.  | 3.7                      | 30                       |
| 36 | Combined Photoredox and Iron Catalysis for the Cyclotrimerization of Alkynes. Angewandte Chemie -<br>International Edition, 2020, 59, 13473-13478.  | 13.8                     | 47                       |

| #  | Article   | IF   | CITATIONS |
|----|---|------|-----------|
| 37 | Interfacial studies in CNT fibre/TiO2 photoelectrodes for efficient H2 production. Applied Catalysis B:<br>Environmental, 2020, 268, 118613.  | 20.2 | 16        |
| 38 | Understanding Charge Transfer Mechanism on Effective Truxene-Based Porous<br>Polymers–TiO <sub>2</sub> Hybrid Photocatalysts for Hydrogen Evolution. ACS Applied Energy<br>Materials, 2020, 3, 4411-4420.   | 5.1  | 29        |
| 39 | Hierarchical Co <sub>3</sub> O <sub>4</sub> nanorods anchored on nitrogen doped reduced<br>graphene oxide: a highly efficient bifunctional electrocatalyst for rechargeable Zn–air batteries.<br>Catalysis Science and Technology, 2020, 10, 1444-1457. | 4.1  | 13        |
| 40 | Ferrite Materials for Photoassisted Environmental and Solar Fuels Applications. Topics in Current Chemistry Collections, 2020, , 107-162.   | 0.5  | 7         |
| 41 | Influence of Post-Synthesis Modifications of Ti1â^'xZrxO2 Nanocrystallites on Their Photocatalytic<br>Activity for Toluene and Methylcyclohexane Degradation. Journal of Nanoscience and<br>Nanotechnology, 2019, 19, 7810-7818.                        | 0.9  | 1         |
| 42 | New Concepts for Production of Scalable Single Layer Oxidized Regions by Local Anodic Oxidation of Graphene. Small, 2019, 15, 1902817.  | 10.0 | 4         |
| 43 | Hydroxamate Titanium–Organic Frameworks and the Effect of Siderophore-Type Linkers over Their<br>Photocatalytic Activity. Journal of the American Chemical Society, 2019, 141, 13124-13133.   | 13.7 | 73        |
| 44 | Conjugated porous polymer based on BOPHY dyes as photocatalyst under visible light. Applied<br>Catalysis B: Environmental, 2019, 258, 117933.   | 20.2 | 46        |
| 45 | 2D Materials Oxidation: New Concepts for Production of Scalable Single Layer Oxidized Regions by Local Anodic Oxidation of Graphene (Small 40/2019). Small, 2019, 15, 1970217.  | 10.0 | 1         |
| 46 | Carbon nanotube synthesis and spinning as macroscopic fibers assisted by the ceramic reactor tube.<br>Scientific Reports, 2019, 9, 9239.  | 3.3  | 28        |
| 47 | Demonstrator devices for artificial photosynthesis: general discussion. Faraday Discussions, 2019, 215, 345-363.  | 3.2  | 2         |
| 48 | Synthetic approaches to artificial photosynthesis: general discussion. Faraday Discussions, 2019, 215, 242-281.   | 3.2  | 5         |
| 49 | Chromoselective access to Z- or E- allylated amines and heterocycles by a photocatalytic allylation reaction. Nature Communications, 2019, 10, 2634.  | 12.8 | 38        |
| 50 | Mesityl or Imide Acridinium Photocatalysts: Accessible Versus Inaccessible Chargeâ€∎ransfer States in<br>Photoredox Catalysis. ChemPhotoChem, 2019, 3, 609-612.   | 3.0  | 8         |
| 51 | Correcting Flaws in the Assignment of Nitrogen Chemical Environments in N-Doped Graphene. Journal of Physical Chemistry C, 2019, 123, 11319-11327.  | 3.1  | 33        |
| 52 | Hybrid materials based on conjugated polymers and inorganic semiconductors as photocatalysts:<br>from environmental to energy applications. Chemical Society Reviews, 2019, 48, 5454-5487.  | 38.1 | 228       |
| 53 | High rate hybrid MnO <sub>2</sub> @CNT fabric anodes for Li-ion batteries: properties and a lithium storage mechanism study by <i>in situ</i> synchrotron X-ray scattering. Journal of Materials Chemistry A, 2019, 7, 26596-26606.                     | 10.3 | 43        |
| 54 | Photoelectrochemical Hydrogen Evolution Driven by Visible-to-Ultraviolet Photon Upconversion.<br>ACS Applied Energy Materials, 2019, 2, 207-211.  | 5.1  | 41        |

| #  | Article   | IF   | CITATIONS |
|----|---|------|-----------|
| 55 | A Facile Synthesis of Blue Luminescent [7]Helicenocarbazoles Based on Goldâ€Catalyzed<br>Rearrangementâ€lodonium Migration and Suzuki–Miyaura Benzannulation Reactions. Chemistry - A<br>European Journal, 2018, 24, 7620-7625. | 3.3  | 11        |
| 56 | Influence of surface density on the CO2 photoreduction activity of a DC magnetron sputtered TiO2 catalyst. Applied Catalysis B: Environmental, 2018, 224, 912-918.  | 20.2 | 30        |
| 57 | Dichromatic Photocatalytic Substitutions of Aryl Halides with a Small Organic Dye. Chemistry - A<br>European Journal, 2018, 24, 105-108.  | 3.3  | 113       |
| 58 | Unravelling the effect of charge dynamics at the plasmonic metal/semiconductor interface for CO2 photoreduction. Nature Communications, 2018, 9, 4986.  | 12.8 | 168       |
| 59 | Mechanistic View of the Main Current Issues in Photocatalytic CO <sub>2</sub> Reduction. Journal of Physical Chemistry Letters, 2018, 9, 7192-7204.   | 4.6  | 76        |
| 60 | Covalent organic nanosheets for bioimaging. Chemical Science, 2018, 9, 8382-8387.   | 7.4  | 84        |
| 61 | Synchronized biphotonic process triggering C C coupling catalytic reactions. Applied Catalysis B:<br>Environmental, 2018, 237, 18-23.   | 20.2 | 38        |
| 62 | A Bifunctional Photoaminocatalyst for the Alkylation of Aldehydes: Design, Analysis, and Mechanistic<br>Studies. ACS Catalysis, 2018, 8, 5928-5940.   | 11.2 | 46        |
| 63 | On the selectivity of CO2 photoreduction towards CH4 using Pt/TiO2 catalysts supported on mesoporous silica. Applied Catalysis B: Environmental, 2018, 239, 68-76.  | 20.2 | 98        |
| 64 | Sulfur polyconjugated organic ligands as building block in photoactive metal–organic frameworks.<br>Acta Crystallographica Section A: Foundations and Advances, 2018, 74, e372-e373.  | 0.1  | 0         |
| 65 | Elucidating the Photoredox Nature of Isolated Iron Active Sites on MCM-41. ACS Catalysis, 2017, 7, 1646-1654.   | 11.2 | 19        |
| 66 | Effect of La as Promoter in the Photoreduction of CO2 Over TiO2 Catalysts. Topics in Catalysis, 2017, 60, 1119-1128.  | 2.8  | 9         |
| 67 | Addressed realization of multication complex arrangements in metal-organic frameworks. Science Advances, 2017, 3, e1700773.   | 10.3 | 47        |
| 68 | CO2 reduction over NaNbO3 and NaTaO3 perovskite photocatalysts. Photochemical and Photobiological Sciences, 2017, 16, 17-23.  | 2.9  | 76        |
| 69 | Metal–organic frameworks based on conjugated organic ligands for optoelectronic applications.<br>Acta Crystallographica Section A: Foundations and Advances, 2017, 73, C202-C202.   | 0.1  | 0         |
| 70 | Hierarchical TiO 2 nanofibres as photocatalyst for CO 2 reduction: Influence of morphology and phase composition on catalytic activity. Journal of CO2 Utilization, 2016, 15, 24-31.  | 6.8  | 61        |
| 71 | Factors influencing the photocatalytic activity ofÂalkali Nb Ta perovskites for hydrogen production from aqueous methanol solutions. International Journal of Hydrogen Energy, 2016, 41, 19921-19928.                           | 7.1  | 11        |
| 72 | Ga-Promoted Photocatalytic H2 Production over Pt/ZnO Nanostructures. ACS Applied Materials &<br>Interfaces, 2016, 8, 23729-23738.   | 8.0  | 43        |

| #  | Article  | IF               | CITATIONS           |
|----|--|------------------|---------------------|
| 73 | Crystal phase competition by addition of a second metal cation in solid solution metal–organic frameworks. Dalton Transactions, 2016, 45, 4327-4337.   | 3.3              | 13                  |
| 74 | Photocatalytic H2 production from aqueous methanol solutions using metal-co-catalysed Zn2SnO4 nanostructures. Applied Catalysis B: Environmental, 2016, 191, 106-115.  | 20.2             | 20                  |
| 75 | Ce-promoted Ni/SBA-15 catalysts for anisole hydrotreating under mild conditions. Applied Catalysis B:<br>Environmental, 2016, 197, 206-213.  | 20.2             | 37                  |
| 76 | Role of the physicochemical properties of hausmannite on the hydrogen production via the<br>Mn3O4–NaOH thermochemical cycle. International Journal of Hydrogen Energy, 2016, 41, 113-122.  | 7.1              | 15                  |
| 77 | Mixed NaNb <sub>x</sub> Ta <sub>1â^'x</sub> O <sub>3</sub> perovskites as photocatalysts for<br>H <sub>2</sub> production. Green Chemistry, 2015, 17, 1735-1743.   | 9.0              | 28                  |
| 78 | Influence of the Ni/P ratio and metal loading on the performance of NixPy/SBA-15 catalysts for the hydrodeoxygenation of methyl oleate. Fuel, 2015, 144, 60-70.  | 6.4              | 70                  |
| 79 | Current Challenges of CO2 Photocatalytic Reduction Over Semiconductors Using Sunlight. , 2015, , 171-191.  |                  | 7                   |
| 80 | Transition Metal Phosphide Nanoparticles Supported on SBA-15 as Highly Selective<br>Hydrodeoxygenation Catalysts for the Production of Advanced Biofuels. Journal of Nanoscience and<br>Nanotechnology, 2015, 15, 6642-6650.                         | 0.9              | 12                  |
| 81 | Effect of Au surface plasmon nanoparticles on the selective CO2 photoreduction to CH4. Applied Catalysis B: Environmental, 2015, 178, 177-185.   | 20.2             | 94                  |
| 82 | Effect of metal–support interaction on the selective hydrodeoxygenation of anisole to aromatics<br>over Ni-based catalysts. Applied Catalysis B: Environmental, 2014, 145, 91-100.   | 20.2             | 192                 |
| 83 | Localization and Impact of Pb-Non-Bonded Electronic Pair on the Crystal and Electronic Structure of Pb2YSbO6. Inorganic Chemistry, 2014, 53, 5609-5618.  | 4.0              | 6                   |
| 84 | Enhancing Metal–Organic Framework Net Robustness by Successive Linker Coordination Increase:<br>From a Hydrogen-Bonded Two-Dimensional Supramolecular Net to a Covalent One Keeping the<br>Topology. Crystal Growth and Design, 2014, 14, 5227-5233. | 3.0              | 36                  |
| 85 | Thermochemical energy storage at high temperature via redox cycles of Mn and Co oxides: Pure oxides versus mixed ones. Solar Energy Materials and Solar Cells, 2014, 123, 47-57.   | 6.2              | 137                 |
| 86 | Photocatalytic hydrogen production in the water/methanol system using Pt/RE:NaTaO3 (REÂ=ÂY, La, Ce,) Tj ETQc   | 0.00 rgB1<br>7:1 | [  Qverlock ]<br>43 |
| 87 | Enhancement of hydrocarbon production via artificial photosynthesis due to synergetic effect of Ag supported on TiO2 and ZnO semiconductors. Chemical Engineering Journal, 2013, 224, 128-135.   | 12.7             | 63                  |
| 88 | H2 production by CH4 decomposition over metallic cobalt nanoparticles: Effect of the catalyst activation. Applied Catalysis A: General, 2013, 467, 371-379.  | 4.3              | 16                  |
| 89 | Advances in the design of ordered mesoporous materials for low-carbon catalytic hydrogen production. Journal of Materials Chemistry A, 2013, 1, 12016.   | 10.3             | 33                  |

Influence of structural and morphological characteristics onÂtheÂhydrogen production and sodium recovery in the NaOH–MnO thermochemical cycle. International Journal of Hydrogen Energy, 2013, 38, 7.1 17 13143-13152.

| #   | Article   | IF   | CITATIONS |
|-----|---|------|-----------|
| 91  | Effect of copper on the performance of ZnO and ZnO1â^'xNx oxides as CO2 photoreduction catalysts.<br>Catalysis Today, 2013, 209, 21-27.   | 4.4  | 62        |
| 92  | H3O2 Bridging Ligand in a Metal–Organic Framework. Insight into the Aqua-Hydroxo↔Hydroxyl<br>Equilibrium: A Combined Experimental and Theoretical Study. Journal of the American Chemical<br>Society, 2013, 135, 5782-5792.   | 13.7 | 42        |
| 93  | Hydrocarbons production through hydrotreating of methyl esters over Ni and Co supported on<br>SBA-15 and Al-SBA-15. Catalysis Today, 2013, 210, 81-88.  | 4.4  | 94        |
| 94  | The Role of Co-catalysts: Interaction and Synergies with Semiconductors. Green Energy and Technology, 2013, , 195-216.  | 0.6  | 1         |
| 95  | Green Microwave Synthesis of MILâ€100(Al, Cr, Fe) Nanoparticles for Thinâ€Film Elaboration. European<br>Journal of Inorganic Chemistry, 2012, 2012, 5165-5174.  | 2.0  | 176       |
| 96  | Insight into the SBU Condensation in Mg Coordination and Supramolecular Frameworks: A Combined Experimental and Theoretical Study. Journal of the American Chemical Society, 2012, 134, 4762-4771.                            | 13.7 | 24        |
| 97  | Synthesis of Nickel Phosphide Nanorods as Catalyst for the Hydrotreating of Methyl Oleate. Topics in Catalysis, 2012, 55, 991-998.  | 2.8  | 22        |
| 98  | Insight into the Correlation between Net Topology and Ligand Coordination Mode in New Lanthanide<br>MOFs Heterogeneous Catalysts: A Theoretical and Experimental Approach. Crystal Growth and Design,<br>2012, 12, 5535-5545. | 3.0  | 45        |
| 99  | Ni <sub>2</sub> P/SBA-15 As a Hydrodeoxygenation Catalyst with Enhanced Selectivity for the<br>Conversion of Methyl Oleate Into <i>n</i> -Octadecane. ACS Catalysis, 2012, 2, 592-598.  | 11.2 | 160       |
| 100 | Mild temperature hydrogen production by methane decomposition over cobalt catalysts prepared with different precipitating agents. International Journal of Hydrogen Energy, 2012, 37, 7034-7041.                              | 7.1  | 27        |
| 101 | VALORIZACION DE CO2. Â; RESIDUO O MATERIA PRIMA?. Dyna (Spain), 2012, 87, 145-148.  | 0.2  | 3         |
| 102 | Co-production of graphene sheets and hydrogen by decomposition of methane using cobalt based catalysts. Energy and Environmental Science, 2011, 4, 778.   | 30.8 | 36        |
| 103 | Direct evidence of the SMSI decoration effect: the case of Co/TiO2 catalyst. Chemical Communications, 2011, 47, 7131.   | 4.1  | 87        |
| 104 | Heterogeneous Catalysis with Alkalineâ€Earth Metalâ€Based MOFs: A Green Calcium Catalyst.<br>ChemCatChem, 2010, 2, 147-149.   | 3.7  | 68        |
| 105 | Electronic and magnetic structure of bulk cobalt: The α, β, and ε-phases from density functional theory calculations. Journal of Chemical Physics, 2010, 133, 024701.   | 3.0  | 83        |
| 106 | Dynamic Calcium Metal–Organic Framework Acts as a Selective Organic Solvent Sponge. Chemistry - A<br>European Journal, 2010, 16, 11632-11640.   | 3.3  | 53        |
| 107 | Cobalt based catalysts prepared by Pechini method for CO2-free hydrogen production by methane decomposition. International Journal of Hydrogen Energy, 2010, 35, 10285-10294.   | 7.1  | 68        |
| 108 | Thermodynamic and Kinetic Control on the Formation of Two Novel Metal-Organic Frameworks Based on the Er(III) Ion and the Asymmetric Dimethylsuccinate Ligand. Inorganic Chemistry, 2010, 49, 5063-5071.                      | 4.0  | 30        |

| #   | Article   | IF   | CITATIONS |
|-----|---|------|-----------|
| 109 | Kinetics and selectivity of methyl-ethyl-ketone combustion in air over alumina-supported PdOx–MnOx catalysts. Journal of Catalysis, 2009, 261, 50-59.   | 6.2  | 45        |
| 110 | Methyl ethyl ketone combustion over La-transition metal (Cr, Co, Ni, Mn) perovskites. Applied Catalysis<br>B: Environmental, 2009, 92, 445-453.   | 20.2 | 54        |
| 111 | Development of Hexagonal Closed-Packed Cobalt Nanoparticles Stable at High Temperature. Chemistry of Materials, 2009, 21, 5637-5643.  | 6.7  | 81        |
| 112 | The role of the Pb2+ 6s lone pair in the structure of the double perovskite Pb2ScSbO6. Dalton Transactions, 2009, , 5453.   | 3.3  | 22        |
| 113 | Three Lanthanum MOF Polymorphs: Insights into Kinetically and Thermodynamically Controlled Phases. Inorganic Chemistry, 2009, 48, 4707-4713.  | 4.0  | 56        |
| 114 | Palladium-manganese catalysts supported on monolith systems for methane combustion. Applied<br>Catalysis B: Environmental, 2008, 79, 122-131.   | 20.2 | 30        |
| 115 | Evidence for spontaneous CO2 activation on cobalt surfaces. Chemical Physics Letters, 2008, 454, 262-268.   | 2.6  | 76        |
| 116 | Catalytic behaviour of bifunctional pumice-supported and zeolite/pumice hybrid catalysts for n-pentane hydroisomerization. Applied Catalysis A: General, 2008, 350, 38-45.                        | 4.3  | 13        |
| 117 | Development of robust Co-based catalysts for the selective H2-production by ethanol<br>steam-reforming. The Fe-promoter effect. International Journal of Hydrogen Energy, 2008, 33,<br>3601-3606. | 7.1  | 48        |
| 118 | Synergistic effect of Pd in methane combustion PdMnO /Al2O3 catalysts. Catalysis Communications, 2007, 8, 1287-1292.  | 3.3  | 40        |
| 119 | Catalytic behaviour of Pt or Pd metal nanoparticles–zeolite bifunctional catalysts for n-pentane<br>hydroisomerization. Catalysis Communications, 2007, 8, 2081-2086.                             | 3.3  | 17        |
| 120 | A Molecule-Based Nanoporous Material Showing Tuneable Spin-Crossover Behavior near Room<br>Temperature. Advanced Materials, 2007, 19, 1397-1402.  | 21.0 | 83        |
| 121 | Fischer–Tropsch synthesis on mono- and bimetallic Co and Fe catalysts in fixed-bed and slurry reactors. Applied Catalysis A: General, 2007, 326, 65-73.   | 4.3  | 103       |
| 122 | X-ray diffraction study of Co3O4 activation under ethanol steam-reforming. Catalysis Today, 2007, 126, 148-152.   | 4.4  | 85        |
| 123 | Spin transition in a triazine-based Fe(ii) complex: variable-temperature structural, thermal, magnetic and spectroscopic studies. Journal of Materials Chemistry, 2006, 16, 2669-2676.            | 6.7  | 36        |
| 124 | TD-DFT analysis of the electronic spectra of Ti-containing catalysts. Topics in Catalysis, 2006, 41, 27-34.   | 2.8  | 23        |
| 125 | Structural changes and activation treatment in a Co/SiO2 catalyst for Fischer–Tropsch synthesis.<br>Catalysis Today, 2006, 114, 422-427.  | 4.4  | 51        |
| 126 | Surface and Structural Features of Co-Fe Oxide Nanoparticles Deposited on a Silica Substrate.<br>European Journal of Inorganic Chemistry, 2006, 2006, 5057-5068.                                  | 2.0  | 50        |

| #   | Article   | IF   | CITATIONS |
|-----|---|------|-----------|
| 127 | Influence of feed composition on the activity of Mn and PdMn/Al2O3 catalysts for combustion of formaldehyde/methanol. Applied Catalysis B: Environmental, 2005, 57, 191-199.  | 20.2 | 101       |
| 128 | Strong dependence on pressure of the performance of a Co/SiO2 catalyst in Fischer–Tropsch slurry reactor synthesis. Catalysis Letters, 2005, 100, 105-116.  | 2.6  | 33        |
| 129 | Formaldehyde/methanol combustion on alumina-supported manganese-palladium oxide catalyst.<br>Applied Catalysis B: Environmental, 2004, 51, 83-91.   | 20.2 | 128       |
| 130 | Synthesis of bis[N,O-{2′-pyridyl-methanolate}]dioxomolybdenum(VI) epoxidation catalyst and novel crystal structure derived from X-ray diffraction and DFT calculations. Journal of Molecular Catalysis A, 2004, 214, 269-272. | 4.8  | 23        |
| 131 | Strong enhancement of the Fischer–Tropsch synthesis on a Co/SiO2 catalyst activate in syngas mixture. Catalysis Communications, 2004, 5, 635-638.   | 3.3  | 34        |
| 132 | Unusually High Selectivity to C2+ Alcohols on Bimetallic CoFe Catalysts During CO Hydrogenation.<br>Catalysis Letters, 2003, 88, 123-128.   | 2.6  | 46        |
| 133 | The Usefulness of Time-Dependent Density Functional Theory to Describe the Electronic Spectra of Ti-Containing Catalysts. Angewandte Chemie - International Edition, 2003, 42, 5851-5854.                                     | 13.8 | 42        |
| 134 | DFT study of electronic spectra and excited-state properties of some 1,8-naphthalimide derivatives.<br>International Journal of Quantum Chemistry, 2003, 91, 446-450.   | 2.0  | 11        |
| 135 | Alumina-supported manganese- and manganese–palladium oxide catalysts for VOCs combustion.<br>Catalysis Communications, 2003, 4, 223-228.  | 3.3  | 126       |
| 136 | The Usefulness of Density Functional Theory To Describe the Tautomeric Equilibrium of<br>4,6-Dimethyl-2-mercaptopyrimidine in Solution. Journal of Physical Chemistry A, 2003, 107, 7490-7495.                                | 2.5  | 35        |
| 137 | Effect of the TiO 2 Nanocrystal Dispersion Over SBAâ€15 in the Photocatalytic H 2 Production Using Ethanol as Electron Donor. Advanced Sustainable Systems, 0, , 2100133.   | 5.3  | 9         |